Received: 14 February 2023 | Revised: 16 June 2023 | Accepted: 22 June 2023

DOI: 10.1002/glia.24437

GLIA

WILEY

RESEARCH ARTICLE

Lipopolysaccharide augments microglial GABA uptake by increasing GABA transporter-1 trafficking and bestrophin-1 expression

Michael Di Palma[1] | Myriam Catalano[2] | Carmela Serpe[2] | Mariassunta De Luca[2] | Lucia Monaco[2] | Karl Kunzelmann[3] | Cristina Limatola[2,4] | Fiorenzo Conti[1,5,6] | Giorgia Fattorini[1,5]

[1]Department of Experimental and Clinical Medicine, Section of Neuroscience and Cell Biology, Università Politecnica delle Marche, Ancona, Italy

[2]Department of Physiology and Pharmacology, Sapienza University of Rome, Rome, Italy

[3]Physiological Institute, University of Regensburg, Regensburg, Germany

[4]IRCCS Neuromed, Pozzilli, Italy

[5]Center for Neurobiology of Aging, INRCA IRCCS, Ancona, Italy

[6]Fondazione di Medicina Molecolare, Università Politecnica delle Marche, Ancona, Italy

Correspondence
Giorgia Fattorini, Department of Experimental and Clinical Medicine, Section of Neuroscience and Cell Biology, Università Politecnica delle Marche, Ancona 60026, Italy.
Email: g.fattorini@univpm.it; g.fattorini@inrca.it

Funding information
Ministero della Salute, Grant/Award Number: RF-2018-12366215; Ministero dell'Università e della Ricerca, Grant/Award Numbers: PRIN 2010/2011: 2010JFYFY2_006, PRIN 2015: 2015E8EMCM, PRIN 2020: 2020Z73J5A; PNRR: RomeTechnopoleFlagship7

Abstract

Gamma-aminobutyric acid (GABA), the principal inhibitory neurotransmitter in the brain, affects numerous immune cell functions. Microglia, the brain's resident innate immune cells, regulate GABA signaling through GABA receptors and express the complete GABAergic machinery for GABA synthesis, uptake, and release. Here, the use of primary microglial cell cultures and ex vivo brain tissue sections allowed for demonstrating that treatment with lipopolysaccharide (LPS) increased microglial GABA uptake as well as GABA transporter (GAT)-1 trafficking. This effect was not entirely abolished by treatment with GAT inhibitors (GAT-Is). Notably, LPS also induced microglial upregulation of bestrophin-1 (BEST-1), a Ca^{2+}-activated Cl^- channel permeable to GABA. Combined administration of GAT-Is and a BEST-1 inhibitor completely abolished LPS-induced microglial GABA uptake. Interestingly, increased microglial GAT-1 membrane turnover via syntaxin 1A was detected in LPS-treated cultures after BEST-1 blockade. Altogether, these findings provided evidence for a novel mechanism through which LPS may trigger the inflammatory response by directly altering microglial GABA clearance and identified the GAT-1/BEST-1 interplay as a potential novel mechanism involved in brain inflammation.

KEYWORDS
bestrophin-1, GABA, GABA transporter 1, inflammation, LPS, microglial cells

1 | INTRODUCTION

Microglial cells, the brain resident mononuclear phagocytes, account for between 5% and 20% of the glial cell population, depending on the region (Colonna & Butovsky, 2017; Pelvig et al., 2008). They constitute the brain's innate immune cell population and act as sentinels, detecting signals of invasion or tissue damage (Ginhoux et al., 2013; Ginhoux & Prinz, 2015; Thion et al., 2018). Under inflammatory conditions, they are involved in repair processes, thus limiting central nervous system (CNS) damage and playing a crucial

Michael Di Palma and Myriam Catalano contributed equally to this study.

role in the pathophysiology of numerous CNS diseases (Colonna & Butovsky, 2017). Such a highly dynamic role is underpinned by their ability to undergo morphological changes, migrate, and perform phagocytosis (Davalos et al., 2005; Nimmerjahn et al., 2005), as well as to switch from housekeeping (Kettenmann et al., 2011, 2013) to adaptive response functions (Colonna & Butovsky, 2017).

Gamma-aminobutyric acid (GABA), the main inhibitory neurotransmitter in the brain (Cherubini & Conti, 2001), is a critical immunomodulator that influences the release of cytokines, phagocytosis, proliferation, and electrophysiological properties of immune cells (Bhandage & Barragan, 2021). Since microglial cells express the complete GABAergic machinery (Bhandage et al., 2019; Bhandage & Barragan, 2021), they synthesize, release, and take up GABA through GABA metabolizing enzyme (GABA-T), GABA-A/B receptors (Lee et al., 2011), and GABA transporters (GATs) 1 and 3 (Fattorini, Catalano, et al., 2020). Su and colleagues have documented a reciprocal influence between the GABAergic system and microglia, showing that production of the pro-inflammatory cytokines interleukin (IL)-1β and tumor necrosis factor (TNF)-α upregulates GAT-1 and GAT-3 brain expressions (Su et al., 2015). Almost at the same time, Liu and coworkers demonstrated that a selective GAT-1 inhibitor, tiagabine (Borden et al., 1994), modulated microglial activities in a mouse model of Parkinson's disease (Liu et al., 2015). Then, at a time when most interactions among microglial cells and the GABAergic system were held to be mediated by neurons and/or astrocytes, our group documented that microglial cells express GATs, highlighting a direct role of microglia as GABA level tuners (Fattorini, Catalano, et al., 2020). These findings suggest that the reciprocal influence of the GABAergic system and microglia may be involved in modulating the local inflammatory response to acute or chronic adverse stimuli.

A widely used mouse model of peripheral inflammation is treatment with lipopolysaccharide (LPS), an endotoxin derived from the outer membrane of gram-negative bacteria, which causes brain inflammation and induces an inflamed microglial phenotype, as seen in human sepsis (Lemstra et al., 2007; Qin et al., 2007). In animal models, LPS treatment also triggers the production of several markers of neurodegenerative disorders, such as Parkinson's disease (Qin et al., 2007), inducing the release of pro-inflammatory cytokines by microglial cells as well as the overexpression of cyclooxygenase-2 and inducible nitric oxide synthase (iNOS) (Catorce & Gevorkian, 2016; Hoogland et al., 2015).

To gain a clearer understanding of the interaction between GABA system and microglia during inflammation, we tested the hypothesis that LPS-induced inflammation affects GAT-1-dependent microglial GABA uptake.

2 | MATERIALS AND METHODS

2.1 | Animals and tissue preparation

Pup and adult C57BL6 wild type and cx3cr1$^{+/gfp}$ mice were used for gene expression, immunofluorescence, and functional studies. Their care and handling were approved by the local animal research ethics committee. Experiments were approved by the Italian Ministry of Health, in accordance with European Directive 2010/63EU and Italian legislative decree 26/2014 on the protection of animals used for scientific purposes, and by the local veterinary service. Animals were kept under a 12-h dark–light cycle with free access to food and water. Mice (8–16 weeks) received an intraperitoneal injection of LPS (from *Escherichia coli* O55:B5, Sigma-Aldrich, Milano, Italy, 1 mg/kg) (Jung et al., 2000). After 24 h, they were deeply anesthetized and perfused transcardially with a flush of saline followed by freshly depolymerized 4% paraformaldehyde in phosphate buffered saline (PBS; 0.1 M). The brains were removed, postfixed in the same fixative for 2–24 h at 4°C, and cut with a vibratome into 20–40 μm thick sections for immunofluorescence studies. For gene expression investigations, animals were deeply anesthetized and perfused transcardially with a flush of phosphate buffer (PB); after the brains had been removed, CD11b^{+} cells were isolated (Grimaldi et al., 2016) and lysed in Trizol reagent (Invitrogen, Milano, Italy) for RNA extraction and PCR analysis.

2.2 | Antibodies

The sources, concentrations, and characterization data of the antibodies used in the study are listed in Table 1.

2.3 | Isolation of CD11b^{+} cells

Brain tissue was digested with trypsin (0.25 mg/mL). The tissue suspension was placed in a 30 μm cell strainer, labeled with CD11b MicroBeads (Miltenyi Biotec, Calderara di Reno, Italy), and isolated according to the manufacturer's instructions.

2.4 | Microglial cultures

Mixed cortical glia cultures were obtained from p0 to p1 mice, whose cerebral cortices were chopped and digested in 20 U/mL papain for 40 min at 37°C. Cells (5–105 cells/cm^2) were plated on dishes coated with poly-L-lysine (100 mg/mL) in DMEM supplemented with 10% fetal bovine serum, 100 U/mL penicillin, and 0.1 mg/mL streptomycin. After 7–9 days, cells were shaken for 2 h at 37°C to detach and collect microglia. These procedures provided almost pure (≤2% contamination) microglial cell populations (Lauro et al., 2010). Cells were then treated with LPS (100 ng/mL) for 24 h.

2.5 | Western blotting

Western blot experiments were carried out on lysates of primary microglial cultures and CD11b^{+} cells. The bicinchoninic acid (BCA) protein assay (Thermo Fisher Scientific, Waltham, MA, USA) and a SPECTROstar Nano microplate reader (BMG Labtech, Ortenberg,

TABLE 1 Primary and secondary antibodies.

Primary antibodies					
Antibodies	**Host**	**Dilution**	**Source**	**Characterization**	**RRID**
GAT-1	R	1:200 (IF, isPLA); 1:500 (WB)	Kindly provided by Dr. N.C. Brecha (Department of Neurobiology, UCLA, Los Angeles, CA, USA)	Minelli et al. (1995), Guo et al. (2009)	AB_2313748
GAT-3	R	1:100 (IF)	Kindly provided by Dr. N.C. Brecha (Department of Neurobiology, UCLA, Los Angeles, CA, USA)	Minelli et al. (1995), Guo et al. (2009)	AB_2313749
STX1A	M	N/A (isPLA)	Synaptic System, Göttingen, Germany/110111	Varoqueaux et al. (2002)	AB_887848
BEST-1	R	1:750 (IF)	Kindly provided by Prof. K. Kunzelmann (Institute of Physiology, Universität Regensburg, Regensburg, Germany)	Barro Soria et al. (2009)	N/A

Secondary antibodies				
Conjugated to	**React**	**Dilution**	**Source**	**RRID**
Cy™3	R	1:250	Jackson ImmunoResearch, West Grove, PA/711-166-152 USA	AB_2313568
Duolink® PLA Probemaker—Plus	N/A	1:40	Sigma-Aldrich/DUO92009-1KT	N/A
Duolink® PLA Probemaker—Minus	N/A	1:40	Sigma-Aldrich/DUO92010-1KT	N/A
Peroxidase	R	1:1000	Jackson ImmunoResearch/711036-152	AB_2340590

Abbreviations: IF, immunofluorescence; isPLA, in situ Proximity Ligation Assay; M, mouse; R; rabbit; WB, western blotting.

Germany) were used to determine the total amount of protein in each lysate (3–4 measurements per lysate). As housekeeping proteins (such as α-actin and β-tubulin) are sensitive to experimental treatments (particularly to pharmacologic treatments) and several physiological conditions, and have therefore some limitations as internal standards (Ferguson et al., 2005), 3–6 measurements were made for each sample. To minimize procedural variables, homogenates from treated and control experimental groups were loaded onto the same gel (Bragina et al., 2006; Marcotulli et al., 2017). Lysates were resolved by SDS–PAGE. Proteins were separated on 4%–15% polyacrylamide gels (Mini-PROTEAN® TGX™ Precast Gels, Bio-Rad Laboratories GmbH, Munchen, Germany). Stain-Free imaging was performed using ChemiDoc MP Imager (Bio-Rad) and Image Lab 4 software (Bio-Rad) with a 5 min stain activation time, and total protein images were therefore obtained. Proteins were then transferred to 0.2 μm nitrocellulose sheet (Midi Nitrocellulose Transfer Kit, Bio-Rad) using Trans-Blot Turbo Transfer System (Bio-Rad). The quality of transfer was controlled by imaging membranes using Stain-Free technology. For quantitative analysis, we drew standard curves of increasing concentration of total protein from controls to define a linear range for immunoblot densitometric analysis (Bragina et al., 2006); for optimal resolution, western blotting studies were performed in primary cultures lysates with 25 μg of total proteins and 10 μg for $CD11b^+$ cells. Nitrocellulose membranes were finally probed with primary antibody at dilution as reported in Table 1. After exposure to appropriate secondary antibodies (Table 1), bands were visualized by Bio-Rad Chemidoc and Image Lab 4 software using the Clarity™ Western ECL (Bio-Rad) chemiluminescent substrate (Bragina et al., 2006). Quantitation of immunoreactive bands was performed using Image Lab 4 (Bio-Rad) and Stain-Free total protein amount technology was used for protein normalization.

2.6 | Immunofluorescence

Cortical brain sections and microglial cells from $cx3cr1^{+/gfp}$ mice (the strain used to visualize microglia) were incubated for 1 h in 10% normal donkey serum (NDS) in PB and then in primary antibodies (GAT-1 or bestrophin [BEST]-1), for 2 h at room temperature and then overnight at 4°C (Table 1). The next day, samples were incubated for 30 min in 10% NDS in PB and subsequently in a mixture of appropriate secondary fluorescent antibodies (Table 1). They were then mounted, air-dried, and coverslipped using Vectashield mounting medium (H-1000; Vector Laboratories, Burlingame, CA). Images were acquired using a Leica SP2 confocal microscope (Leica Microsystems, Wetzlar, Germany). Samples incubated only with the secondary antibody, used as control, revealed no cross-reactivity.

2.7 | In situ proximity ligation assay

Microglial cells were used for direct in situ proximity ligation assays (isPLAs) (Alam, 2018; Borroto-Escuela et al., 2011; Borroto-Escuela et al., 2013, 2016; Di Palma et al., 2020). Custom is PLA probes were created (Alam, 2018) using Duolink PLA Probemaker kit (Sigma-Aldrich) according to the manufacturer's instructions. Primary antibodies (1 mg/mL; Table 1) were used to create the Plus and Minus isPLA probes (GAT1 and syntaxin 1A [STX1A], respectively). The experiments were then performed according to the manufacturer's protocol.

2.8 | Reverse transcription-PCR

Total RNA was extracted from primary microglia and $CD11b^+$ cells using Trizol reagent. DNA contamination was removed by treatment

TABLE 2 Qrt-PCR primer sequences.

Gene	Forward	Reverse
Gapdh	TCGTCCCGTAGACAAAATGG	TTGAGGTCAATGAAGGGGTC
Cx3cr1	TGACTGGCACTTCCTGCAGA	AGGGCGTAGAAGACGGACAG
Il1b	GCAACTGTTCCTGAACTCAACT	GCAACTGTTCCTGAACTCAACT
Cd86	AGAACTTACGGAAGCACCCA	AGAACTTACGGAAGCACCCA
Tnfα	GTGGAACTGGCAGAAGAG	CCATAGAACTGATGAGAGG
Gat-1	TAACAACAACAGCCCATCCA	GGAGTAACCCTGCTCCATGA
Best-1[a]	GGATCTGGTTGTGCCTGTCT	AAGTTCTGGTGCATCCCATC

[a]Best-1 validated primer sequences (Jo et al., 2014).

with DNase I (Invitrogen), according to the manufacturer's recommendations. RNAs extracted from all samples were quantified and reverse transcribed using Iscript Reverse Transcription Supermix (Bio-Rad, Munchen, Germany). The products were used as templates for PCR amplification. PCR was carried out in an MJ-Mini-Personal Thermal Cycler (Bio-Rad) using Dream Taq Green PCR Master Mix (Thermo Scientific, Monza, Italy). The reagents were added to the reaction tubes according to the manufacturer's instructions, and primers were added at a final concentration of 0.5 mM. The primer sequences for Best-1, cx3cr1, and Gapdh are reported in Table 2. Gapdh was used as a loading control and Cx3cr1 as a microglia marker. The PCR reaction was as follows: 95°C for 75 s, 62°C for 30 s, 35 cycles of 72°C for 45 s, and a final extension step at 72°C for 15 min. The amplification product was analyzed on 1.5% agarose gel and photographed under an ultraviolet transilluminator.

2.9 | Real-time reverse transcription-PCR

Real-Time Quantitative Reverse Transcription PCR (RT-qPCR) was performed in an iCycler iQ Multi-Color Real Time PCR Detection System using SsoAdvanced Universal SYBR Green Supermix (both from Bio-Rad). The PCR protocol consisted of 40 cycles of denaturation at 95°C for 30 s and annealing/extension at 58°C for 30 s. The Ct values of each gene were normalized to the Ct value of Gapdh in the same RNA sample (ΔCt). Relative quantification was performed using the $2^{-\Delta\Delta Ct}$ method and expressed as fold increase. The primer sequence details are reported in Table 2.

3 | DATA COLLECTION AND ANALYSIS

3.1 | Confocal microscopy and 3D IMARIS reconstruction

GAT-1, BEST-1, and GAT-1-STX1A (isPLA) immunofluorescence from mouse brain sections and cx3cr1$^{+/gfp}$ microglial cells were analyzed with a Leica SP2 TCS-SL confocal microscope. For 3D reconstruction, Z-stack images (9–30 µm depth, 0.87–1.36 µm steps) were acquired with a planapo 63× objective (numerical aperture 1.4, pinhole 1.0, image size 512 × 512 pixels, yielding a frame of 79.35 µm). Signal acquisition was optimized; photomultiplier gain was set so that the brightest pixels were just slightly below saturation and offset such that the darkest pixels were just above zero. To avoid bleed-through between green and red fluorescence, images were acquired sequentially. To improve the signal/noise ratio, 8–10 frames/image were averaged. Raw LEI files were used for further analysis using Bitplane IMARIS software (v. 7.4.2, Oxford Instruments, Schlieren, Switzerland). First, the software was used to reconstruct the microglial, GAT-1, BEST-1, and isPLA product surfaces using an optimized custom setting for each target. After surface reconstruction, the filter function was applied to remove non-specific background signal. All microglia with incomplete somata were manually removed using the cut function and excluded from further analysis. All images contained at least three microglial cells per field. Fused microglia falsely recognized as one entity by the software were manually separated using the cut function or removed from the sample if the separation was not feasible. For the brain sections, further processing steps were employed to explore microglial complexity and microglia-GAT-1 and microglia-BEST-1 colocalization and topography (Figure S1). Cell complexity was assessed by Sholl analysis. To do this, the microglial surface was used as a template for filament reconstruction adopting the default settings. Seed points were manually corrected, either placed in or removed from the center of the soma if the IMARIS algorithm placed them incorrectly. The filament reconstructions were used to compute the total number of Sholl intersections per microglial cell. Microglial complexity was evaluated as the total number of Sholl intersections and peak number for Sholl intersections (computed as the sum of all intersections/microglial cell) and as peak number for Sholl intersections per microglial cell (the highest numerical value of a sphere intersecting a microglial process) (Althammer et al., 2020). Topographical analyses between the microglial center of mass and colocalized surfaces were performed using the "distance transformation" extension (Figure S2). The extension was also used to compute the distance between the cell surface and intracellular surfaces (GAT-1, BEST-1, or isPLA products) in microglial cell cultures. Finally, all surfaces and filament parameters were exported to separate Excel files and used for data and statistical analysis. Image processing, 3D reconstruction, and data analysis were always performed blindly.

3.2 | [^{3}H]-GABA uptake assays

The uptake of [^{3}H]-GABA was evaluated as described previously (Fattorini, Catalano, et al., 2020). To identify the more suitable time point for inhibitor application, that is, the first time point with a significant uptake variation compared to the control condition, primary microglial cells were incubated with [^{3}H]-GABA (0.1 mM) and GABA (10 mM) for 5–60 min at 37°C in saline solution containing 140 mM NaCl, 5 mM KCl, 2 mM $MgCl_2$, 2 mM $CaCl_2$, 10 mM HEPES, and glucose 4.5 g/L (pH 7.4) or in Na^+-free buffer, where sodium was replaced with an equimolar concentration of choline. Inhibitors of GAT-1 (NNC-711, 1 mM), GAT-2/3 (SNAP-5114, 100 mM, both from Tocris Bioscience), BEST-1 (NPPB, 100 mM), and STX1A (BoNT/C1, 1 ng/mL) were added at appropriate time points as specified in the relevant figure captions. Samples were tested for radioactivity and protein content was evaluated by BCA assay. The uptake rate for each well was expressed as pCi of [^{3}H]-GABA per µg of protein. Data obtained in Na^+-free buffer were subtracted from treated samples. Data were obtained from at least three independent experiments.

3.3 | Statistical analysis

Data distribution was explored using the Shapiro–Wilk normality test to establish whether parametric or non-parametric statistics were appropriate. The homoscedasticity/homogeneity of variance means was examined using Levene's test. Data were analyzed using GraphPad Prism 9 (GraphPad Software, San Diego, CA, USA). Significance was accepted at $p < .05$. The statistical design for each analysis is detailed in the corresponding figure legend.

4 | RESULTS

4.1 | LPS treatment affects microglial GABA uptake

mRNA analysis of LPS-treated primary microglial cells demonstrated a significant increase in the expression of Il1β and iNos pro-inflammatory genes (Figure S3), in line with the phenotype known to be elicited by this treatment (Golia et al., 2019; Hoogland et al., 2015). To determine whether the neuroinflammatory response affects microglial Gat-1 expression and function, control (CTRL) and LPS-treated cells were subjected to Qrt-PCR, western blotting, and morphological and functional analyses.

LPS treatment did not affect Gat-1 gene expression (fold change: CTRL = 1 ± 0.01 vs. LPS = 1.19 ± 0.15; Figure 1a, inset), and GAT-1 total protein amount assessed by western blotting analyses (fold change: CTRL = 100 ± 16.93 vs. LPS = 121.7 ± 15.12; Figure S4). However, immunofluorescence data revealed a significant increase in GAT-1 expression when normalized to cell volume upon LPS treatment compared to CTRL (% of cell volume: CTRL = 1.40 ± 0.47 vs. LPS = 2.63 ± 0.46; $p = .04$; Figure 1a–c and Figure S5).

Since GAT-1/STX1A interaction is crucial in regulating GAT-1 membrane expression (Fattorini, Catalano, et al., 2020; Quick, 2002; Quick et al., 1997), we used isPLA analysis to quantify GAT-1/STX1A heterocomplexes. We found that LPS-treated cells showed (i) a significant increase of GAT-1/STX1A heterocomplexes/cell (LPS = 21.63 ± 1.63; CTRL = 12.96 ± 2.70 isPLA products/cell; $p = .02$; Figure 2a–c and Figure S6), and (ii) a significantly shorter distance of the heterocomplexes from the cell membrane (peak distance from plasma membrane: LPS = 0.4 µm vs. CTRL = 1.4 µm; Figure 2d). A radiolabeled transmitter uptake assay, performed to determine

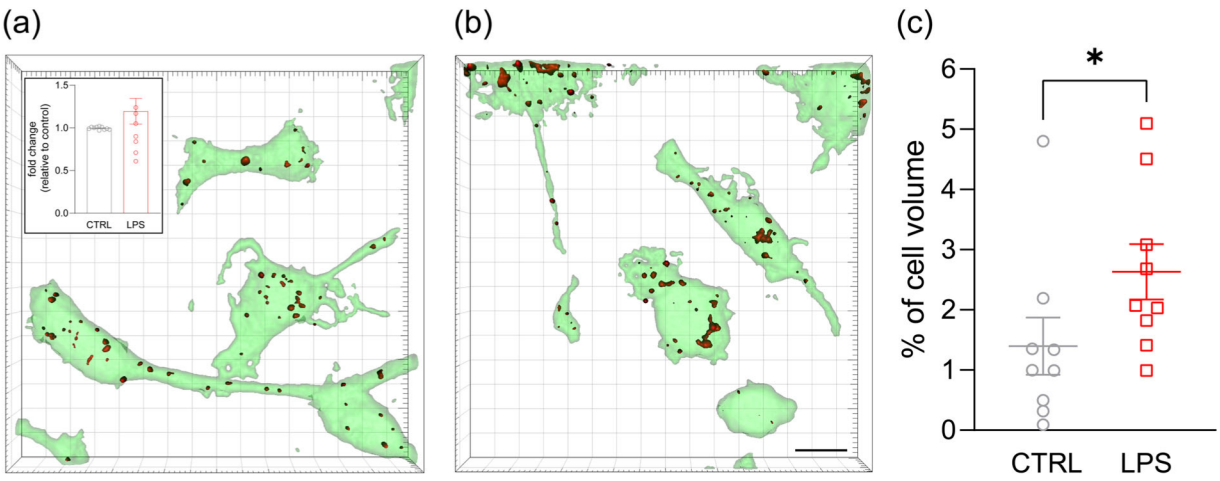

FIGURE 1 Localization of GAT-1 immunoreactivity in control and LPS-treated cx3cr1$^{+/gfp}$ primary microglial cell cultures. Qrt-PCR of Gat-1 gene in primary microglial cells (a, inset, $N = 10$). Representative 3D surface volume reconstructions of cx3cr1$^{+/gfp}$ microglial cells (green) and GAT-1 staining (red) in control (a) and LPS-treated (b) cultures. Percentage of cell volume colocalized with GAT-1 staining in control (gray) and LPS-treated (red) cells (c; Mann–Whitney $U = 17$, $^*p = .04$, $N = 9$). Data are expressed as mean ± SEM. Scale bar: 10 µm.

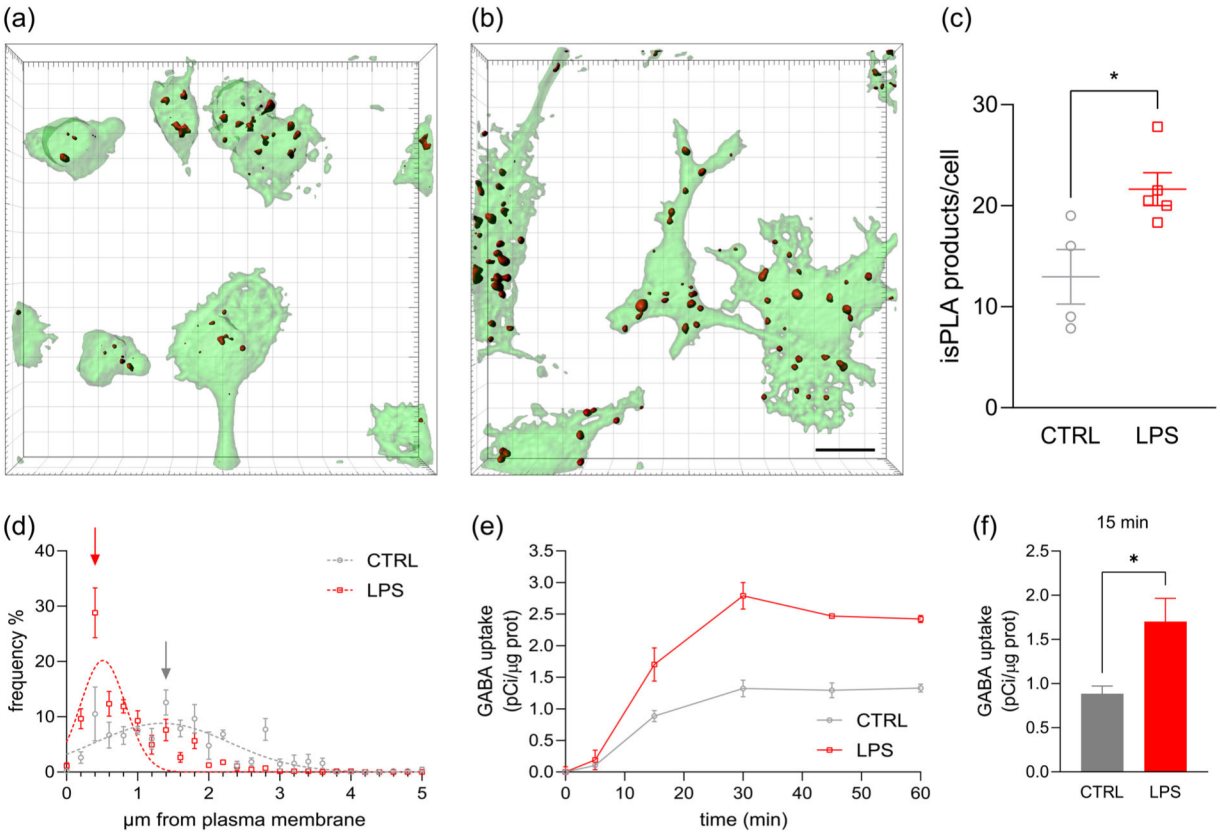

FIGURE 2 Effect of lipopolysaccharide (LPS) treatment on microglial GAT-1 expression and gamma-aminobutyric acid (GABA) uptake. Representative 3D surface volume reconstructions of cx3cr1$^{+/gfp}$ microglial cells (green) and GAT-1-STX1A heterocomplexes (red) in control (a) and LPS-treated (b) cells. Quantitative analysis of GAT-1-STX1A heterocomplexes expressed as number of positive isPLA products per cell (isPLA products/cell) in control (gray) and LPS-treated (red) cells (c; unpaired student's *t*-test $t = 2.884$, df $= 7$, $^*p = .02$, CTRL $N = 4$ and LPS $N = 5$). Percent frequency distribution of GAT-1-STX1A heterocomplexes as a function of the intracellular distance from the cell surface (µm from plasma membrane). Arrows indicate the CTRL (gray) and LPS (red) data distribution peaks. Dashed line represents non-linear fit for CTRL (gray) and LPS-treated (red) cells (d; Gaussian-fit different curve for each data-set, $F = 28.27$, DFn $= 3$, DFd $= 228$, $p < .001$). Time course of Na^+-dependent GABA uptake in CTRL (gray) and LPS-treated (red) cells (e; Kruskal-Wallis test $\chi^2 = 123$, $p < .001$). Na^+-dependent GABA uptake in CTRL (gray) and LPS-treated (red) cells at 15 min (f; data represent GABA uptake as pCi/µg of protein, CTRL: 0.89 ± 0.09, $N = 38$; LPS: 1.70 ± 0.27, $N = 26$, Mann–Whitney $U = 336$, $^*p = .03$). Data are expressed as mean ± SEM. Scale bar: 10 µm.

whether the increased GAT-1 expression was paralleled by increased microglial GABA uptake, demonstrated significantly increased Na^+-dependent GABA uptake (192.08 ± 29.91% compared to CTRL; $p = .03$) 15 min after LPS treatment (Figure 2e,f).

4.2 | The LPS-induced GABA uptake increase is partly mediated by GATs

To establish whether the LPS-induced increase in GABA uptake was GAT-mediated, we conducted radiolabeled transmitter uptake assays using selective inhibitors of GAT-1 and GAT-2/3, respectively NNC-711 and SNAP-5114 (Borden, 1996; Borden et al., 1994; Fattorini, Catalano, et al., 2020) (Figure 3a). In line with our previous work (Fattorini, Catalano, et al., 2020), we found that in untreated cultures the GAT-Is reduced GABA uptake by 80% compared to CTRL at 15 min ($p = .039$; Figure 3b), whereas in LPS-treated cells the reduction was only 60% ($p < .001$; Figure 3b).

These findings suggest the action of a GAT-independent mechanism on GABA uptake in LPS-treated cells.

4.3 | The LPS-induced GABA uptake increase involves BEST-1

The Ca^{2+}-activated Cl^- channel BEST-1 is permeable to GABA (Kwak et al., 2020; Lee et al., 2010), and microglial cells express BEST-1 transcript (Bhandage et al., 2019; Song et al., 2020). We, therefore, investigated whether BEST-1 contributes to LPS-induced GAT-independent microglial GABA uptake.

We first confirmed that primary microglial cells express Best-1 mRNA, and actually extended previous findings (Bhandage et al., 2019; Song et al., 2020) by demonstrating BEST-1 protein expression in both primary microglial cells and isolated CD11b + cells (Figure 4a,b). In primary microglial cells, LPS treatment significantly increased Best-1 mRNA levels (fold change: CTRL = 1 ± 0.01

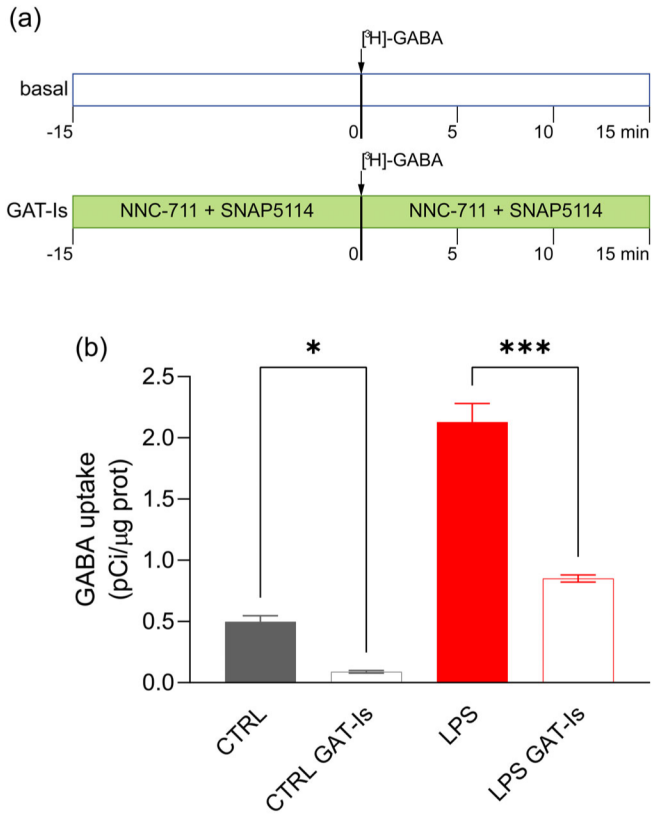

FIGURE 3 Lipopolysaccharide (LPS)-induced non-GAT-mediated gamma-aminobutyric acid (GABA) uptake in microglial cells. Treatment scheme of microglial cell cultures with the GAT-Is. Na^+-dependent GABA uptake (basal: white box, blue line) in presence of NNC-711, a selective GAT-1 inhibitor, and of SNAP-5114, a selective GAT-2/3 inhibitor; green box, GAT-Is) (a). Data represent GABA uptake as pCi/µg of protein at 15 min in CTRL (gray) and LPS-treated (red) cultures; Kruskal-Wallis test $\chi^2 = 76.13$, $p < .001$, Dunn's post hoc pairwise comparison $^*p = .039$; $^{***}p < .001$ (b; CTRL: 0.50 ± 0.05, $N = 19$; CTRL GAT-Is: 0.09 ± 0.01, $N = 18$; LPS: 2.13 ± 0.15, $N = 19$; LPS + GAT-Is: 0.85 ± 0.03, $N = 32$). Data are expressed as mean ± SEM.

vs. LPS = 2.60 ± 0.46; $p < .001$; Figure 5a), and protein expression (% of cell volume: CTRL = 1.11 ± 0.36 vs. LPS = 2.94 ± 0.64; $p = .03$; Figure 5b–d inset), and reduced the distance of BEST-1 protein from the cell surface (distribution peak distance: CTRL = 1 µm vs. LPS = 0.4 µm; Figure 5d).

Next, to determine whether BEST-1 mediates GABA influx into LPS-treated microglial cells, we measured radiolabeled transmitter uptake using both the GAT-Is and the BEST-1 inhibitor NPPB (Kwak et al., 2020; Lee et al., 2010) (Figure 6a). In untreated cultures, GABA uptake was not affected by NPPB and there were no significant differences between GAT-Is and NPPB+GAT-Is cultures (GAT-Is: 14.70 ± 1.40%; NPPB: 107.70 ± 9.63%; NPPB+GAT-Is: 23.10 ± 2.84% vs. CTRL at 15 min; Figure 6b), suggesting negligible BEST-1 plasma membrane expression in these conditions. In LPS-treated cells, GABA uptake was unaffected by NPPB (81.73 ± 6.55% compared to LPS at 15 min, Figure 6c); however, use of NPPB+GAT-Is virtually abolished GABA uptake, thus removing all residual GAT-independent uptake (NPPB+GAT-Is: 6.88 ± 0.62% vs. LPS at 15 min; LPS vs. NPPB+GAT-Is, $p < .001$; GAT-Is vs. NPPB, $p < .001$; GAT-Is vs. NPPB+GAT-Is, $p = .001$; Figure 6c).

In a previous work, we showed that inhibition of non-GAT-1-mediated GABA uptake leads to increased microglial STX1A/GAT-1 membrane expression (Fattorini, Catalano, et al., 2020). The negligible GABA uptake measured in the NPPB+GAT-Is cultures suggested to us that, in LPS-treated microglial cultures, BEST-1 inhibition may increase STX1A/GAT-1 membrane expression, thus accounting for the unchanged GABA uptake measured in NPPB experimental group. To test this hypothesis, we used botulinum toxin C1 (BoNT/C1), which specifically cleaves STX1A (Deken et al., 2000; Schiavo et al., 1995). Indeed, BoNT/C1 strongly reduced the effect of NPPB on GABA uptake (36.63 ± 2.636% compared to NPPB in basal condition at 15 min, $p = .033$; Figure 6d), and completely abolished it when BoNT/C1 was followed by GAT-Iss (6.01 ± 0.678% compared NPPB in basal condition at 15 min vs. NPPB + BoNT/C1, $p = .033$; Figure 6d), indicating that in LPS-treated microglia GABA uptake was sustained almost equally by GATs and BEST-1.

4.4 | LPS affects GAT-1 cellular distribution profile in microglia in vivo

Next, we evaluated whether GAT-1 and BEST-1 expression in mice is modulated by LPS treatment. To assess the efficacy of LPS treatment, mRNA analysis was carried out in microglial cells ($CD11b^+$) isolated from untreated (CTRL) and LPS-treated mice. A significant increase of Il1β, Cd86, and Tnfα transcripts, detected in cells from LPS-treated mice (Figure 7a), confirmed treatment efficacy. LPS treatment also altered cortical microglia morphology, as evaluated by Sholl analysis (Althammer et al., 2020), since 3D quantitative morphometric analysis showed significantly reduced peak number (Figure 7b) and total number of Sholl intersections (Figure 7c) in LPS-treated mice compared to controls. In addition, a Sholl analysis plot (Figure 7d) illustrated that the branching profile of LPS-treated microglial cells was shifted to the left, indicating decreased branching as a function of distance from the soma compared to control mice.

Once established that LPS treatment did affect the microglial phenotype, we investigated whether it also impacted gene expression and the cellular distribution of microglial GAT-1 and BEST-1 proteins. In line with the in vitro experiments (Figure 1a), LPS did not affect Gat-1 transcript (Figure 7e), whereas 3D morphometric analysis of microglial cells confirmed a redistribution of GAT-1 immunostaining after LPS treatment, with GAT-1-positive puncta being detected significantly closer to the plasma membrane compared to untreated animals (Figure 7f–h; 0.2 µm from surface in LPS-treated vs. 0.4 µm from the surface in CTRL). LPS treatment also induced a significant increase in Best-1 mRNA, mirroring the data obtained in the primary microglial cultures, whereas BEST-1 immunostaining was not affected (Figure 7j–l). The latter findings demonstrate that LPS treatment modulates GAT-1 and BEST-1 also in vivo.

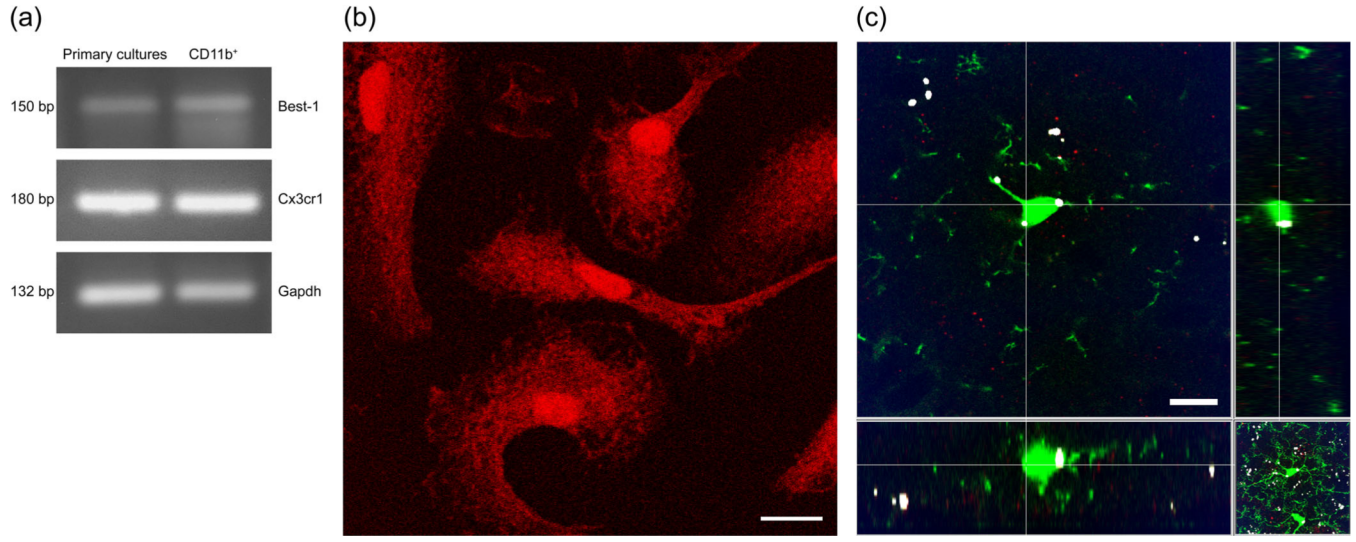

FIGURE 4 BEST-1 expression in primary microglial cells and cx3cr1$^{+/gfp}$ mice. Best-1 mRNA expression in primary microglial cell cultures and in CD11b^{+} cells from adult cx3cr1$^{+/gfp}$ mice. mRNA expression was determined by RT-PCR. Best-1: 150 bp; Cx3cr1: 180 bp; and Gapdh: 132 bp (a). Raw image of a single confocal plane of BEST-1 immunostaining in microglial cultures (b). BEST-1 immunostaining (red: not colocalized puncta; white: colocalized puncta) in brain sections from adult cx3cr1$^{+/gfp}$ mice (c). Scale bar: 10 µm.

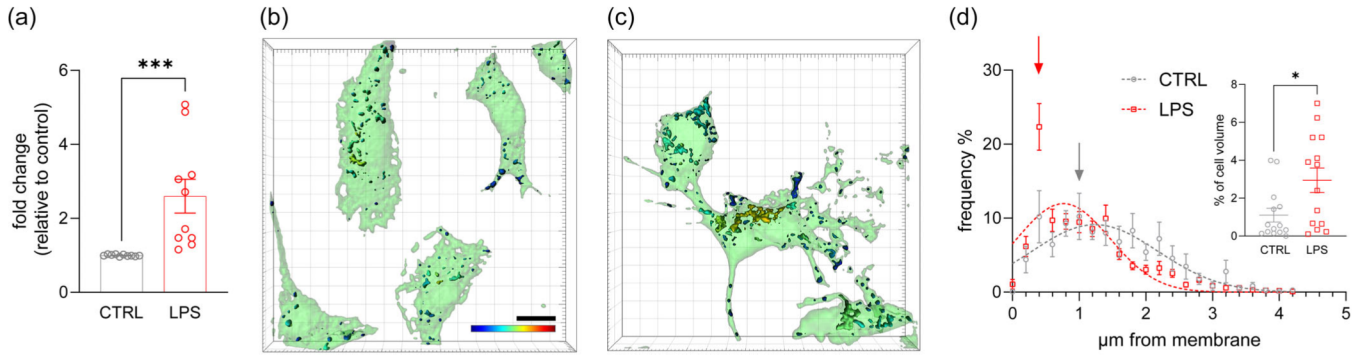

FIGURE 5 Effect of lipopolysaccharide (LPS) treatment on microglial BEST-1 expression. Qrt-PCR of Best-1 gene in primary microglial cells (Mann–Whitney $U = 0$, N = 10, ***$p < .001$; a). Representative 3D surface volume reconstructions of cx3cr1$^{+/gfp}$ microglial cells (green) and BEST-1 (color bar) in control (b) and LPS-treated (c) cells. Percentage of cell volume colocalized with BEST-1 staining in control (gray) and LPS-treated (red) cells (Mann–Whitney $U = 51$, *$p = .031$, $N = 14$; d inset). Percent frequency distribution of BEST-1 immunostaining as a function of the intracellular distance from the surface of cx3cr1$^{+/gfp}$ microglial cells. Arrows indicate the CTRL (gray) and LPS (red) data distribution peaks. Dashed lines represent non-linear fit for CTRL (gray) and LPS (red) conditions (d; Gaussian-fit different curve for each data-set, $F = 10.16$, DFn = 3, DFd = 654, $p < .001$). Data are expressed as mean ± SEM. Scale bar: 10 µm; color bar: 0–4.2 µm from plasma membrane.

5 | DISCUSSION

Our experiments showed that LPS treatment of microglial cells increased microglial GABA uptake, GAT-1 trafficking, and BEST-1 protein expression. They also showed for the first time that GAT-1 membrane trafficking was modulated by BEST-1 inhibition, thus demonstrating a novel functional interplay between the two protomers in microglial GABA signaling regulation in inflammatory conditions.

GABA, the main CNS inhibitory neurotransmitter, plays a critical role in immunomodulation (Bhandage & Barragan, 2021; Crowley et al., 2016; Guyon et al., 2013; Jin et al., 2013; Liu et al., 2016). In the brain, inflammatory conditions, including LPS treatment, induce an excitation-inhibition imbalance (Falco et al., 2014; Garcia-Oscos et al., 2015; Rossi et al., 2011, 2012; Yan et al., 2015), and are associated with reduced GABA signaling (Crowley et al., 2016). One mechanism underpinning reduced GABA signaling in such conditions is the loss of GABA neurons in multiple brain regions (Crowley et al., 2016). The consequent reorganization of the astrocytic and microglial GABAergic machinery also affects the inflammatory response (Lee et al., 2011; Su et al., 2015). For example, microglial production of the pro-inflammatory cytokines IL-1β and TNF-α results in GAT-1 and GAT-3 upregulation in neuronal and glial cells of different brain regions (Su et al., 2015). Although GAT-1 has long been considered as a primarily neuronal transporter, the demonstration that microglial cells are endowed with a complete GABAergic machinery (Bhandage & Barragan, 2021; Bhandage et al., 2019; Lee et al., 2011),

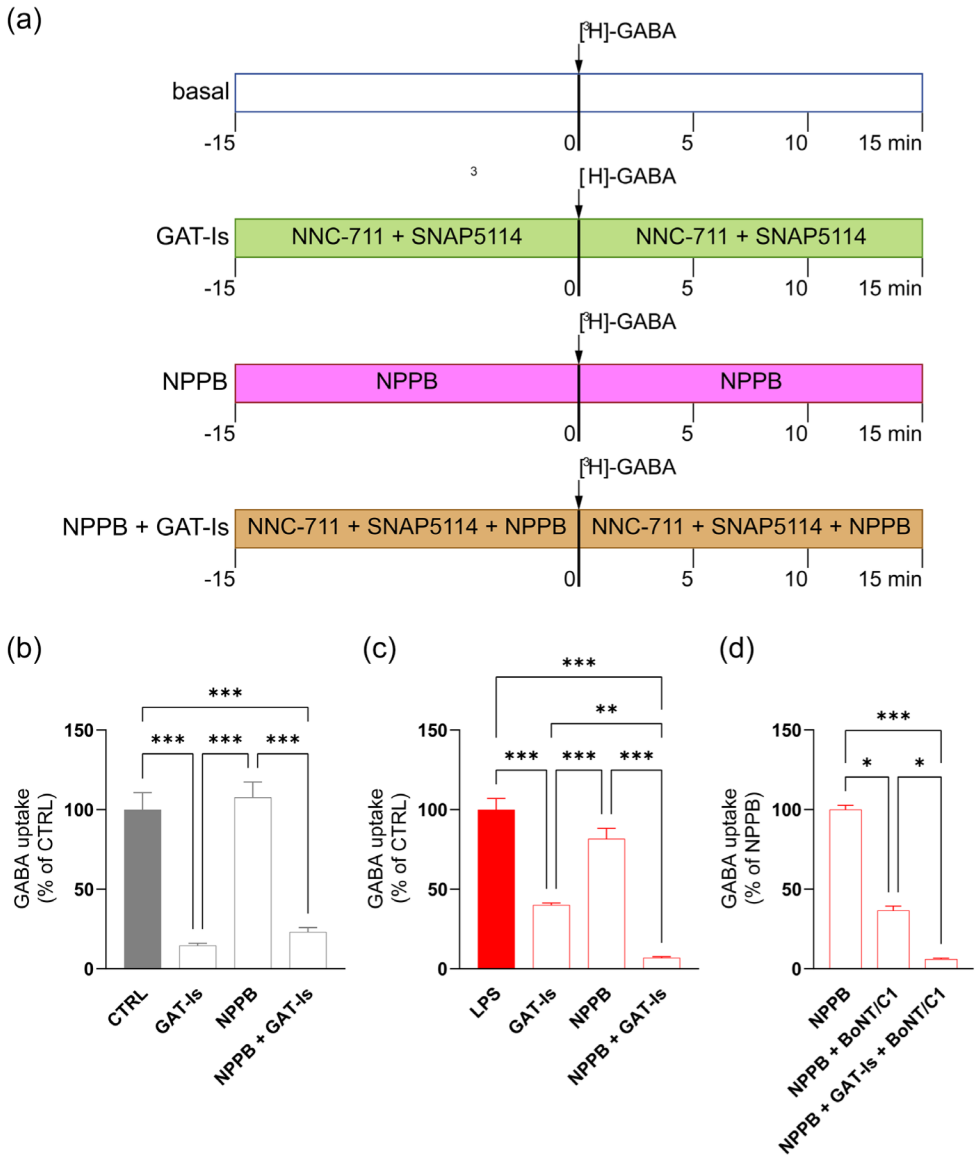

FIGURE 6 Lipopolysaccharide (LPS) induced BEST-1-mediated gamma-aminobutyric acid (GABA) influx in microglial cells. Treatment scheme of microglial cell cultures with the GATs and BEST-1 inhibitors. Na^+-dependent GABA uptake (basal: white box, blue line) in presence of GAT-Is (NNC-711 and SNAP-5114; green box), NPPB (BEST-1 inhibitor, magenta box), and NPPB+GAT-Is (orange box) (a). Data represent % of CTRL uptake at 15 min (b; gray, Kruskal-Wallis test $\chi^2 = 65.61$, $p < .001$, Dunn's post hoc pairwise comparison $^{***}p < .001$, $N = 16–64$) and percent LPS uptake at 15 min (c; red, Kruskal-Wallis test $\chi^2 = 84.01$, $p < .001$, Dunn's post hoc pairwise comparison $^{**}p = .001$; $^{***}p < .001$, $N = 19–66$). GABA uptake at 15 min in microglia cultures treated with LPS and BoNT/C1 in presence of NPPB (NPPB+BoNT/C1) and NPPB +GAT-Is (NPPB+GAT-Is+ BoNT/C1), expressed as percent of microglial culture at basal in presence of NPPB (NPPB) (d; red, Kruskal-Wallis test $\chi^2 = 25.81$, $p < .001$, Dunn's post hoc pairwise comparison $^{*}p = .033$; $^{***}p < .001$, $N = 10$). Data are expressed as mean ± SEM.

including GAT-1 and GAT-3 (Fattorini, Catalano, et al., 2020; Fattorini, Melone, & Conti, 2020), and express functional $GABA_B$ receptors, thus sensing neuronal activity (Favuzzi et al., 2021; Kuhn et al., 2004; Lee et al., 2011; Logiacco et al., 2021), means that the classic GAT-1 "neurocentric view" is no longer tenable (Fattorini et al., 2017; Fattorini, Catalano, et al., 2020; Melone et al., 2015). Here, we postulate a novel mechanism through which LPS may trigger an inflammatory response by directly affecting microglial GABA clearance. In this regard, the LPS-induced increase in GAT-1 trafficking, and the possible consequent reduction in GABA tone, may provide a mechanism that potentiates the inflammatory response, curbing the inhibitory effect of $GABA_B$ activity (Kuhn et al., 2004; Lee et al., 2011).

This notion is supported by the present in vivo findings of increased GAT-1 trafficking to the plasma membrane in neocortical microglial cells after systemic LPS treatment. These data suggest that, by increasing GAT-1 trafficking, LPS sustains the inflammatory response, swamping or hampering the homeostatic action of local environmental signals. In line with this hypothesis, reduced LPS-induced NF-kB activation and nitric oxide production by microglial cells have been described after tiagabine blockade of GAT-1 activity in a mouse model of Parkinson's disease (Liu et al., 2015). Tiagabine also conferred partial protection on the nigrostriatal axis, alleviating the motor deficits, and its protective function was abolished in GAT-1 knockout mice challenged with 1-methyl 4-phenyl 1,2,3,6-tetrahydropyridine (MPTP). Our findings suggest that such protective effects may partially depend on a direct action on microglial GAT-1.

Importantly, the GABAergic signaling modulation described in inflammatory conditions may be region-dependent and cytokine-specific. Indeed, Jiang and coworkers recently reported that acute LPS treatment potentiated the amplitude and frequency of miniature inhibitory postsynaptic currents in glutamatergic neurons of the medial prefrontal cortex (mPFC), it increased microglial cell body size and CD68 expression, and augmented abnormal

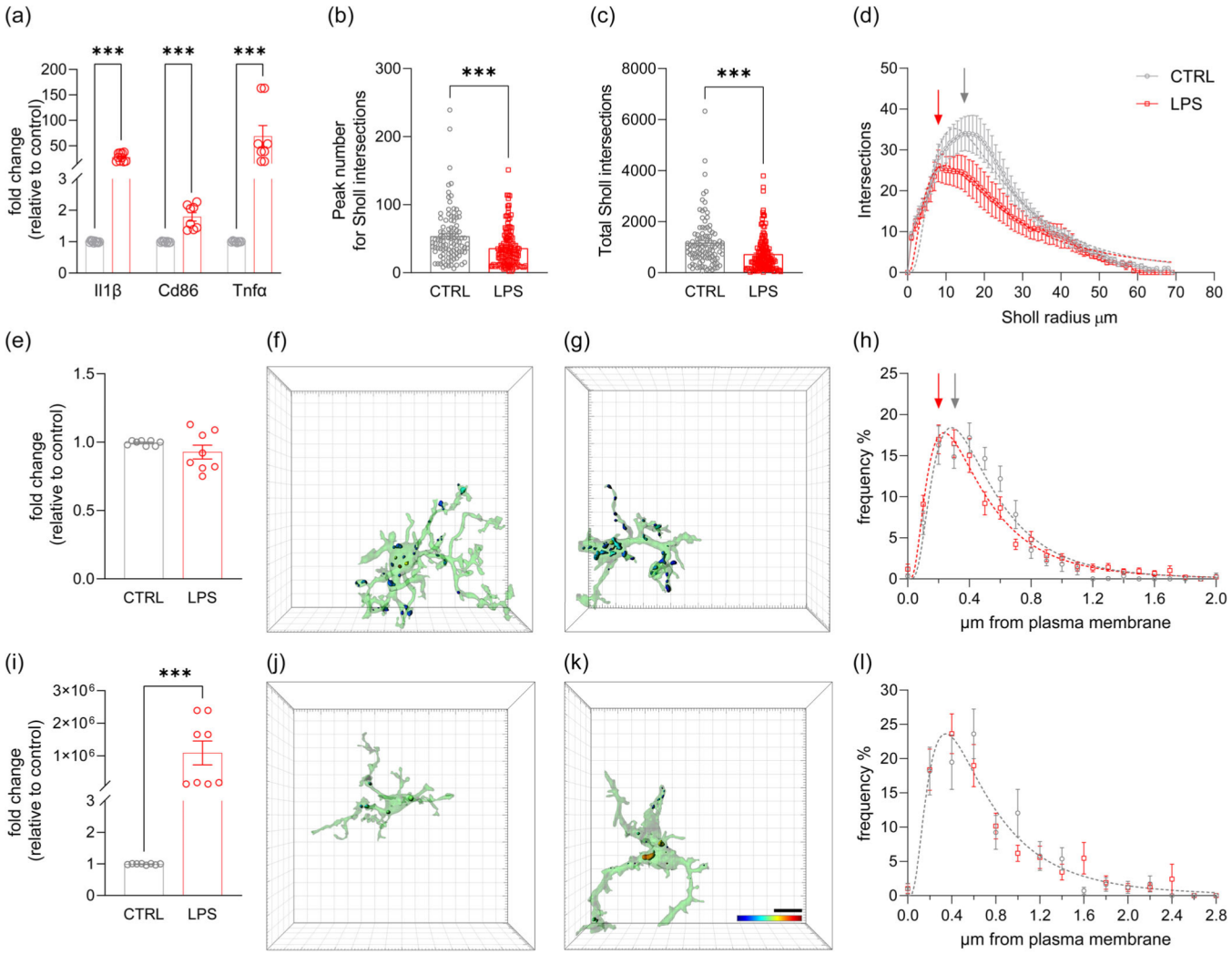

FIGURE 7 Effect of lipopolysaccharide (LPS) treatment on GAT-1 and BEST-1 expression in microglial cells of adult cx3cr1$^{+/gfp}$ mice. Qrt-PCR of Il1-β, Cd86, and Tnf-α genes in CD11b^{+} cells (a; Il-1β, Mann–Whitney $U = 0$, $N = 10$, ***$p < .001$; Cd86, Mann–Whitney $U = 0$, $N = 8$, ***$p < .001$; Tnf-α, Mann–Whitney $U = 0$, $N = 8$, ***$p < .001$). Peak number (b; the highest numerical value of a sphere intersecting a microglial process, CTRL: 53 ± 4 µm, LPS: 36 ± 2 µm, Mann–Whitney $U = 4983$, ***$p < .001$) and total number (c; the sum of all the intersections per individual microglial cell, Mann–Whitney $U = 4713$, ***$p < .001$) of Sholl intersections in CTRL (gray) and LPS-treated (red) conditions. Mean distribution plots of the number of Sholl intersections as a function of the distance from the microglial soma. Arrows indicate the fitting peak for CTRL (gray) and LPS-treated (red) conditions, respectively (d; LogNormal-fit different curve for each data-set, $F = 39.97$, DFn = 3, DFd = 674, $p < .001$). Qrt-PCR of Gat-1 gene in CD11b^{+} cells (e). Representative 3D surface reconstructions of GAT-1 colocalized volume (color bar) with microglial cells (green surfaces) in CTRL (f) and LPS (g) conditions. Percent frequency distribution of GAT-1 (h) immunostaining as a function of the distance from the microglial plasma membrane. Arrows indicate the CTRL (gray) and LPS (red) data distribution peaks. Dashed line represents non-linear fit for CTRL (gray) and LPS-treated (red) conditions (h: Lognormal-fit different curve for each data-set, $F = 8.946$, DFn = 3, DFd = 2008, $p < .001$). Qrt-PCR of Best-1 gene in CD11b^{+} cells (i; Mann–Whitney $U = 0$, $N = 8$, ***$p < .001$). Representative 3D surface reconstructions of BEST-1 (j, k) colocalized volume (color bar) with microglial cells (green surfaces) in CTRL (j) and LPS-treated (k) conditions. Percentage frequency distribution of BEST-1 (l) immunostaining as a function of the distance from the microglial plasma membrane. Dashed line represents non-linear fit for both CTRL (gray) and LPS-treated (red) conditions (l: LogNormal-fit one curve for all data-set, $F = 0.43$, DFn = 3, DFd = 650, $p = .73$). $N = 18$–33 reconstructed cell surfaces from 3 to 4 animals/experimental condition, $N \sim 800$ puncta/experimental condition; data are expressed as mean ± SEM. Scale bar: 10 µm; color bar: 0–2.606 µm from plasma membrane for GAT-1 and 0–2.116 µm from plasma membrane for BEST-1.

exploratory behavior (Jiang et al., 2022). Interestingly, tiagabine pretreatment prevented the effects of LPS on mPFC microglial cells, on behavior, and on GABA signaling, which is consistent with a direct effect on microglial GAT-1. This evidence, combined with the increase in GAT-1 trafficking detected in our LPS-treated microglial cells, suggests a role for microglial GAT-1 trafficking in the inflammatory response.

Unexpectedly, our in vitro functional data showed that the GAT blockade did not completely abolish GABA uptake in LPS-treated microglial cells. This finding suggests the action of a non-

GAT-mediated microglial GABA clearing mechanism, which further strengthens the role of microglia as GABA level tuners in triggering and maintaining neurotransmission as well as the inflammatory response. In several brain areas, astroglial processes are enriched in the GABA-permeable Ca^{2+}-activated Cl^- channel BEST-1 (Lee et al., 2010), which is involved in the fine-tuning of GABA transmission (Kwak et al., 2020; Lee et al., 2010). Also, a transient increase in renal BEST-1 protein expression has been described in LPS-treated animals (Aldehni et al., 2009). Here, we demonstrate that in LPS-treated microglia BEST-1 is involved in non-GAT mediated GABA uptake.

BEST-1 expression and function are related to intracellular calcium transients (Park et al., 2009). LPS activates several toll-like receptors (TLRs; Chung et al., 2010; Olson & Miller, 2004), including TLR4 in microglial cells (Bettoni et al., 2008). Through mitogen-activated protein kinases, TLRs activate a signaling pathway, which in turn results in NF-kB activation (Nicotra et al., 2012; Schroder et al., 2006). Under inflammatory conditions this pathway induces activation of Orai1 (a key member of the calcium release-activated calcium channels; Kraft, 2015) in astrocytes, resulting in increased intracellular calcium levels (Birla et al., 2022). Since microglia also express Orai1, it is conceivable that a similar mechanism modulates the LPS-mediated BEST-1 upregulation (Michaelis et al., 2015).

The GAT-1 membrane turnover is highly dynamic (Horton & Quick, 2001; Quick, 2002) and we have previously described STX1A-mediated microglial GAT-1 trafficking after GAT-3 blockade (Fattorini, Catalano, et al., 2020). Here, we describe how BEST-1 blockade allowed identifying a similar STX1A-mediated mechanism, since our in vitro data showed that the increased membrane permeability to GABA, observed in LPS-treated microglial cells, also triggered a BEST-1/GAT-1 interplay. This finding contributes to unravel the complex modulation of GAT-1 microglial membrane expression in inflammation.

Finally, we provide in vivo evidence that LPS treatment also modulate Best-1 mRNA, albeit not its protein. Even though technical limitations cannot be excluded, intraperitoneal administration of LPS clearly has the potential to induce peripheral effects that modulate the CNS (micro)environment, further differentiating it from in vitro system. These issues need to be addressed if we are to gain further insight into the complex microglial modulation of BEST-1 in inflammation.

AUTHOR CONTRIBUTIONS

Michael Di Palma: Conceptualization, investigation, methodology, data analyses, writing, reviewing and editing. Myriam Catalano: Conceptualization, investigation, methodology, data analyses, writing, reviewing and editing. Carmela Serpe: Methodology, validation, formal analysis, investigation. Mariassunta De Luca: Methodology, formal analysis. Lucia Monaco: Methodology, formal analysis. Karl Kunzelmann: Provided the BEST-1 KO verified antibody. Cristina Limatola: Supervision, conceptualization, reviewing and editing, funding acquisition. Fiorenzo Conti: Supervision, conceptualization, reviewing and editing, funding acquisition. Giorgia Fattorini: Conceptualization, investigation, methodology, data analyses, writing, reviewing and editing, supervision.

ACKNOWLEDGMENTS

This study was supported by funds from Ministero dell'Università e della Ricerca (PRIN 2010/2011: 2010JFYFY2_006) to F.C. and (PRIN 2020: 2020Z73J5A; PRIN 2015: 2015E8EMCM) to C.L. and from Ministero della Salute (RF-2018-12366215) to C.L. The authors are grateful to N.C. Brecha (University of California, Los Angeles) for his generous gift of the GAT antibodies, and to G. Carmignoto and C. Montecucco (University of Padua) for providing the BoNT/Cl protein. Open access funding provided by BIBLIOSAN.

DATA AVAILABILITY STATEMENT

Data sharing is not applicable to this article, as no new data were created or analyzed in this study.

ORCID

Michael Di Palma https://orcid.org/0000-0002-9190-6128
Cristina Limatola https://orcid.org/0000-0001-7504-8197
Fiorenzo Conti https://orcid.org/0000-0001-5853-1566
Giorgia Fattorini https://orcid.org/0000-0002-2497-2942

REFERENCES

Alam, M. S. (2018). Proximity Ligation Assay (PLA). *Curr Protoc Immunol*, *123*(1), e58. https://doi.org/10.1002/cpim.58

Aldehni, F., Spitzner, M., Martins, J. R., Barro-Soria, R., Schreiber, R., & Kunzelmann, K. (2009). Bestrophin 1 promotes epithelial-to-mesenchymal transition of renal collecting duct cells. *J Am Soc Nephrol*, *20*(7), 1556–1564. https://doi.org/10.1681/ASN.2008090987

Althammer, F., Ferreira-Neto, H. C., Rubaharan, M., Roy, R. K., Patel, A. A., Cox, D. N., & Stern, J. E. (2020). Three-dimensional morphometric analysis reveals time-dependent structural changes in microglia and astrocytes in the central amygdala and hypothalamic paraventricular nucleus of heart failure rats. *J Neuro inflammation*, *17*(1), 221. https://doi.org/10.1186/s12974-020-01892-4

Barro Soria, R., Spitzner, M., Schreiber, R., & Kunzelmann, K. (2009). Bestrophin-1 enables Ca2+-activated Cl- conductance in epithelia. *J Biol Chem*, *284*(43), 29405–29412. https://doi.org/10.1074/jbc.M605716200

Bettoni, I., Comelli, F., Rossini, C., Granucci, F., Giagnoni, G., Peri, F., & Costa, B. (2008). Glial TLR4 receptor as new target to treat neuropathic pain: efficacy of a new receptor antagonist in a model of peripheral nerve injury in mice. *Glia*, *56*(12), 1312–1319. https://doi.org/10.1002/glia.20699

Bhandage, A. K., & Barragan, A. (2021). GABAergic signaling by cells of the immune system: more the rule than the exception. *Cell Mol Life Sci*, *78*(15), 5667–5679. https://doi.org/10.1007/s00018-021-03881-z

Bhandage, A. K., Kanatani, S., & Barragan, A. (2019). Toxoplasma-Induced Hypermigration of Primary Cortical Microglia Implicates GABAergic Signaling. *Front Cell Infect Microbiol*, *9*, 73. https://doi.org/10.3389/fcimb.2019.00073

Birla, H., Xia, J., Gao, X., Zhao, H., Wang, F., Patel, S., Amponsah, A., Bekker, A., Tao, Y. X., & Hu, H. (2022). Toll-like receptor 4 activation enhances Orai 1-mediated calcium signal promoting cytokine production in spinal astrocytes. *Cell Calcium*, *105*, 102619. https://doi.org/10.1016/j.ceca.2022.102619

Borden, L. A. (1996). GABA transporter heterogeneity: pharmacology and cellular localization. *Neurochem Int*, *29*(4), 335–356. https://doi.org/10.1016/0197-0186(95)00158-1

Borden, L. A., Murali Dhar, T. G., Smith, K. E., Weinshank, R. L., Branchek, T. A., & Gluchowski, C. (1994). Tiagabine, SK & F 89976-A, CI-966, and NNC-711 are selective for the cloned GABA transporter GAT-1. *Eur J Pharmacol*, *269*(2), 219–224. https://doi.org/10.1016/0922-4106(94)90089-2

Borroto-Escuela, D. O., Hagman, B., Woolfenden, M., Pinton, L., Jiménez-Beristain, A., Oflijan, J., Narvaez, M., Di Palma, M., Feltmann, K., Sartini, S., Ambrogini, P., Ciruela, F., Cuppini, R., & Fuxe, K. (2016). In situ proximity ligation assay to study and understand the distribution and balance of GPCR homo- and hetero receptor complexes in the brain. *In Neuro methods*, *110*, 109-124.

Borroto-Escuela, D. O., Romero-Fernandez, W., Garriga, P., Ciruela, F., Narvaez, M., Tarakanov, A. O., Palkovits, M., Agnati, L. F., & Fuxe, K. (2013). G protein-coupled receptor hetero dimerization in the Brain. *In Methods in Enzymology*, *521*, 281–294.

Borroto-Escuela, D. O., Tarakanov, A. O., Guidolin, D., Ciruela, F., Agnati, L. F., & Fuxe, K. (2011). Moonlighting characteristics of G protein-coupled receptors: focus on receptor heteromers and relevance for neurodegeneration. *IUBMB Life*, *63*(7), 463–472. https://doi.org/10.1002/iub.473

Bragina, L., Melone, M., Fattorini, G., Torres-Ramos, M., Vallejo-Illarramendi, A., Matute, C., & Conti, F. (2006). GLT-1 down-regulation induced by clozapine in rat frontal cortex is associated with synaptophysin up-regulation. *J Neurochem*, *99*(1), 134–141. https://doi.org/10.1111/j.1471-4159.2006.04030.x

Catorce, M. N., & Gevorkian, G. (2016). LPS-induced Murine Neuro inflammation Model: Main Features and Suitability for Pre-clinical Assessment of Nutraceuticals. *Curr Neuropharmacol*, *14*(2), 155–164. https://doi.org/10.2174/1570159x14666151204122017

Cherubini, E., & Conti, F. (2001). Generating diversity at GABAergic synapses. *Trends Neurosci*, *24*(3), 155–162. https://doi.org/10.1016/s0166-2236(00)01724-0

Chung, D. W., Yoo, K. Y., Hwang, I. K., Kim, D. W., Chung, J. Y., Lee, C. H., Choi, J. H., Choi, S. Y., Youn, H. Y., Lee, I. S., & Won, M. H. (2010). Systemic administration of lipopolysaccharide induces cyclooxygenase-2 immuno reactivity in endothelium and increases microglia in the mouse hippocampus. *Cell Mol Neurobiol*, *30*(4), 531–541. https://doi.org/10.1007/s10571-009-9477-0

Colonna, M., & Butovsky, O. (2017). Microglia function in the central nervous system during health and neurodegeneration. *Annu Rev Immunol*, *35*, 441–468. https://doi.org/10.1146/annurev-immunol-051116-052358

Crowley, T., Cryan, J. F., Downer, E. J., & O'Leary, O. F. (2016). Inhibiting neuro inflammation: The role and therapeutic potential of GABA in neuro-immune interactions. *Brain Behav Immun*, *54*, 260–277. https://doi.org/10.1016/j.bbi.2016.02.001

Davalos, D., Grutzendler, J., Yang, G., Kim, J. V., Zuo, Y., Jung, S., Littman, D. R., Dustin, M. L., & Gan, W. B. (2005). ATP mediates rapid microglial response to local brain injury in vivo. *Nat Neurosci*, *8*(6), 752–758. https://doi.org/10.1038/nn1472

Deken, S. L., Beckman, M. L., Boos, L., & Quick, M. W. (2000). Transport rates of GABA transporters: regulation by the N-terminal domain and syntaxin 1A. *Nat Neurosci*, *3*(10), 998–1003. https://doi.org/10.1038/79939

Di Palma, M., Sartini, S., Lattanzi, D., Cuppini, R., Pita-Rodriguez, M., Diaz-Carmenate, Y., Narvaez, M., Fuxe, K., Borroto-Escuela, D. O., & Ambrogini, P. (2020). Evidence for the existence of A2AR-Trk B hetero receptor complexes in the dorsal hippocampus of the rat brain: Potential implications of A2AR and Trk B interplay upon ageing. *Mech Ageing Dev*, *190*, 111289. https://doi.org/10.1016/j.mad.2020.111289

Falco, A., Pennucci, R., Brambilla, E., & De Curtis, I. (2014). Reduction in parvalbumin-positive interneurons and inhibitory input in the cortex of mice with experimental autoimmune encephalomyelitis. *Experimental Brain Research*, *232*(7), 2439–2449. https://doi.org/10.1007/s00221-014-3944-7

Fattorini, G., Catalano, M., Melone, M., Serpe, C., Bassi, S., Limatola, C., & Conti, F. (2020a). Microglial expression of GAT-1 in the cerebral cortex. *Glia*, *68*(3), 646–655. https://doi.org/10.1002/glia.23745

Fattorini, G., Melone, M., & Conti, F. (2020b). A Reappraisal of GAT-1 Localization in Neocortex. *Front Cell Neurosci*, *14*, 9. https://doi.org/10.3389/fncel.2020.00009

Fattorini, G., Melone, M., Sanchez-Gomez, M. V., Arellano, R. O., Bassi, S., Matute, C., & Conti, F. (2017). GAT-1 mediated GABA uptake in rat oligodendrocytes. *Glia*, *65*(3), 514–522. https://doi.org/10.1002/glia.23108

Favuzzi, E., Huang, S., Saldi, G. A., Binan, L., Ibrahim, L. A., Fernandez-Otero, M. M., Cao, Y., Zeine, A., Sefah, A., Zheng, K., Xu, Q., Khlestova, E., Farhi, S. L., Bonneau, R., Datta, S. R., Stevens, B., & Fishell, G. (2021). GABA-receptive microglia selectively sculpt developing inhibitory circuits. *Cell*, *184*(22), 5686. https://doi.org/10.1016/j.cell.2021.10.009

Ferguson, R. E., Carroll, H. P., Harris, A., Maher, E. R., Selby, P. J., & Banks, R. E. (2005). Housekeeping proteins: a preliminary study illustrating some limitations as useful references in protein expression studies. *Proteomics*, *5*(2), 566–571. https://doi.org/10.1002/pmic.200400941

Garcia-Oscos, F., Peña, D., Housini, M., Cheng, D., Lopez, D., Cuevas-Olguin, R., Saderi, N., Salgado Delgado, R., Galindo Charles, L., Salgado Burgos, H., Rose-John, S., Flores, G., Kilgard, M. P., & Atzori, M. (2015). Activation of the anti-inflammatory reflex blocks lipopolysaccharide-induced decrease in synaptic inhibition in the temporal cortex of the rat. *Journal of Neuroscience Research*, *93*(6), 859–865. https://doi.org/10.1002/jnr.23550

Ginhoux, F., Lim, S., Hoeffel, G., Low, D., & Huber, T. (2013). Origin and differentiation of microglia. *Front Cell Neurosci*, *7*, 45. https://doi.org/10.3389/fncel.2013.00045

Ginhoux, F., & Prinz, M. (2015). Origin of microglia: current concepts and past controversies. *Cold Spring Harb Perspect Biol*, *7*(8), a020537. https://doi.org/10.1101/cshperspect.a020537

Golia, M. T., Poggini, S., Alboni, S., Garofalo, S., Ciano Albanese, N., Viglione, A., Ajmone-Cat, M. A., St-Pierre, A., Brunello, N., Limatola, C., Branchi, I., & Maggi, L. (2019). Interplay between inflammation and neural plasticity: Both immune activation and suppression impair LTP and BDNF expression. *Brain Behav Immun*, *81*, 484–494. https://doi.org/10.1016/j.bbi.2019.07.003

Grimaldi, A., D'Alessandro, G., Golia, M. T., Grossinger, E. M., Di Angelantonio, S., Ragozzino, D., Santoro, A., Esposito, V., Wulff, H., Catalano, M., & Limatola, C. (2016). KCa3.1 inhibition switches the phenotype of glioma-infiltrating microglia/macrophages. *Cell Death Dis*, *7*(4), e 2174. https://doi.org/10.1038/cddis.2016.73

Guo, C., Stella, S. L., Jr., Hirano, A. A., & Brecha, N. C. (2009). Plasmalemmal and vesicular gamma-aminobutyric acid transporter expression in the developing mouse retina. *J Comp Neurol*, *512*(1), 6–26. https://doi.org/10.1002/cne.21846

Guyon, A., Kussrow, A., Olmsted, I. R., Sandoz, G., Bornhop, D. J., & Nahon, J. L. (2013). Baclofen and other GABAB receptor agents are allosteric modulators of the CXCL12 chemokine receptor CXCR4. *J Neurosci*, *33*(28), 11643–11654. https://doi.org/10.1523/JNEUROSCI.6070-11.2013

Hoogland, I. C., Houbolt, C., van Westerloo, D. J., van Gool, W. A., & van de Beek, D. (2015). Systemic inflammation and microglial activation: systematic review of animal experiments. *J Neuro inflammation*, *12*, 114. https://doi.org/10.1186/s12974-015-0332-6

Horton, N., & Quick, M. W. (2001). Syntaxin 1A up-regulates GABA transporter expression by subcellular redistribution. *Mol Membr Biol*, *18*(1), 39–44.

Jiang, J., Tang, B., Wang, L., Huo, Q., Tan, S., Misrani, A., Han, Y., Li, H., Hu, H., Wang, J., Cheng, T., Tabassum, S., Chen, M., Xie, W., Long, C., & Yang, L. (2022). Systemic LPS-induced microglial activation results in increased GABAergic tone: A mechanism of protection against neuro inflammation in the medial prefrontal cortex in mice. *Brain Behav Immun*, *99*, 53–69. https://doi.org/10.1016/j.bbi.2021.09.017

Jin, Z., Mendu, S. K., & Birnir, B. (2013). GABA is an effective immunomodulatory molecule. *Amino Acids*, *45*(1), 87–94. https://doi.org/10.1007/s00726-011-1193-7

Jo, S., Yarishkin, O., Hwang, Y. J., Chun, Y. E., Park, M., Woo, D. H., Bae, J. Y., Kim, T., Lee, J., Chun, H., Park, H. J., Lee, D. Y., Hong, J., Kim, H. Y.,

Oh, S. J., Park, S. J., Lee, H., Yoon, B. E., Kim, Y., … Lee, C. J. (2014). GABA from reactive astrocytes impairs memory in mouse models of Alzheimer's disease. *Nat Med*, *20*(8), 886–896. https://doi.org/10.1038/nm.3639

Jung, S., Aliberti, J., Graemmel, P., Sunshine, M. J., Kreutzberg, G. W., Sher, A., & Littman, D. R. (2000). Analysis of fractalkine receptor CX (3) CR1 function by targeted deletion and green fluorescent protein reporter gene insertion. *Mol Cell Biol*, *20*(11), 4106–4114. https://doi.org/10.1128/MCB.20.11.4106-4114.2000

Kettenmann, H., Hanisch, U. K., Noda, M., & Verkhratsky, A. (2011). Physiology of microglia. *Physiol Rev*, *91*(2), 461–553. https://doi.org/10.1152/physrev.00011.2010

Kettenmann, H., Kirchhoff, F., & Verkhratsky, A. (2013). Microglia: new roles for the synaptic stripper. *Neuron*, *77*(1), 10–18. https://doi.org/10.1016/j.neuron.2012.12.023

Kraft, R. (2015). STIM and ORAI proteins in the nervous system. *Channels (Austin)*, *9*(5), 245–252. https://doi.org/10.1080/19336950.2015.1071747

Kuhn, S. A., van Landeghem, F. K., Zacharias, R., Farber, K., Rappert, A., Pavlovic, S., Hoffmann, A., Nolte, C., & Kettenmann, H. (2004). Microglia express GABA (B) receptors to modulate interleukin release. *Mol Cell Neurosci*, *25*(2), 312–322. https://doi.org/10.1016/j.mcn.2003.10.023

Kwak, H., Koh, W., Kim, S., Song, K., Shin, J. I., Lee, J. M., Lee, E. H., Bae, J. Y., Ha, G. E., Oh, J. E., Park, Y. M., Kim, S., Feng, J., Lee, S. E., Choi, J. W., Kim, K. H., Kim, Y. S., Woo, J., Lee, D., … Cheong, E. (2020). Astrocytes Control Sensory Acuity via Tonic Inhibition in the Thalamus. *Neuron*, *108*(4), 691–706 e610. https://doi.org/10.1016/j.neuron.2020.08.013

Lauro, C., Cipriani, R., Catalano, M., Trettel, F., Chece, G., Brusadin, V., Antonilli, L., Van Rooijen, N., Eusebi, F., Fredholm, B. B., & Limatola, C. (2010). Adenosine A1 receptors and microglial cells mediate CX3CL1-induced protection of hippocampal neurons against Glu-induced death. *Neuro psychopharmacology*, *35*(7), 1550–1559. https://doi.org/10.1038/npp.2010.26

Lee, M., Schwab, C., & McGeer, P. L. (2011). Astrocytes are GABAergic cells that modulate microglial activity. *Glia*, *59*(1), 152–165. https://doi.org/10.1002/glia.21087

Lee, S., Yoon, B. E., Berglund, K., Oh, S. J., Park, H., Shin, H. S., Augustine, G. J., & Lee, C. J. (2010). Channel-mediated tonic GABA release from glia. *Science*, *330*(6005), 790–796. https://doi.org/10.1126/science.1184334

Lemstra, A. W., Groen in't Woud, J. C., Hoozemans, J. J., van Haastert, E. S., Rozemuller, A. J., Eikelenboom, P., & van Gool, W. A. (2007). Microglia activation in sepsis: a case-control study. *J Neuro inflammation*, *4*, 4. https://doi.org/10.1186/1742-2094-4-4

Liu, H., Leak, R. K., & Hu, X. (2016). Neurotransmitter receptors on microglia. *Stroke Vasc Neurol*, *1*(2), 52–58. https://doi.org/10.1136/svn-2016-000012

Liu, J., Huang, D., Xu, J., Tong, J., Wang, Z., Huang, L., Yang, Y., Bai, X., Wang, P., Suo, H., Ma, Y., Yu, M., Fei, J., & Huang, F. (2015). Tiagabine Protects Dopaminergic Neurons against Neurotoxins by Inhibiting Microglial Activation. *Sci Rep*, *5*, 15720. https://doi.org/10.1038/srep15720

Logiacco, F., Xia, P., Georgiev, S. V., Franconi, C., Chang, Y. J., Ugursu, B., Sporbert, A., Kühn, R., Kettenmann, H., & Semtner, M. (2021). Microglia sense neuronal activity via GABA in the early postnatal hippocampus. *Cell Rep*, *37*(13), 110128. https://doi.org/10.1016/j.celrep.2021.110128

Marcotulli, D., Fattorini, G., Bragina, L., Perugini, J., & Conti, F. (2017). Levetiracetam Affects Differentially Presynaptic Proteins in Rat Cerebral Cortex. *Front Cell Neurosci*, *11*, 389. https://doi.org/10.3389/fncel.2017.00389

Melone, M., Ciappelloni, S., & Conti, F. (2015). A quantitative analysis of cellular and synaptic localization of GAT-1 and GAT-3 in rat neocortex. *Brain Struct Funct*, *220*(2), 885–897. https://doi.org/10.1007/s00429-013-0690-8

Michaelis, M., Nieswandt, B., Stegner, D., Eilers, J., & Kraft, R. (2015). STIM1, STIM2, and Orai 1 regulate store-operated calcium entry and purinergic activation of microglia. *Glia*, *63*(4), 652–663. https://doi.org/10.1002/glia.22775

Minelli, A., Brecha, N. C., Karschin, C., DeBiasi, S., & Conti, F. (1995). GAT-1, a high-affinity GABA plasma membrane transporter, is localized to neurons and astroglia in the cerebral cortex. *J Neurosci*, *15*(11), 7734–7746.

Nicotra, L., Loram, L. C., Watkins, L. R., & Hutchinson, M. R. (2012). Toll-like receptors in chronic pain. *Exp Neurol*, *234*(2), 316–329. https://doi.org/10.1016/j.expneurol.2011.09.038

Nimmerjahn, A., Kirchhoff, F., & Helmchen, F. (2005). Resting microglial cells are highly dynamic surveillants of brain parenchyma in vivo. *Science*, *308*(5726), 1314–1318. https://doi.org/10.1126/science.1110647

Olson, J. K., & Miller, S. D. (2004). Microglia initiate central nervous system innate and adaptive immune responses through multiple TLRs. *J Immunol*, *173*(6), 3916–3924. https://doi.org/10.4049/jimmunol.173.6.3916

Park, H., Oh, S. J., Han, K. S., Woo, D. H., Park, H., Mannaioni, G., Traynelis, S. F., & Lee, C. J. (2009). Bestrophin-1 encodes for the Ca2+-activated anion channel in hippocampal astrocytes. *J Neurosci*, *29*(41), 13063–13073. https://doi.org/10.1523/JNEUROSCI.3193-09.2009

Pelvig, D. P., Pakkenberg, H., Stark, A. K., & Pakkenberg, B. (2008). Neocortical glial cell numbers in human brains. *Neurobiol Aging*, *29*(11), 1754–1762. https://doi.org/10.1016/j.neurobiolaging.2007.04.013

Qin, L., Wu, X., Block, M. L., Liu, Y., Breese, G. R., Hong, J. S., Knapp, D. J., & Crews, F. T. (2007). Systemic LPS causes chronic neuro inflammation and progressive neurodegeneration. *Glia*, *55*(5), 453–462. https://doi.org/10.1002/glia.20467

Quick, M. W. (2002). Substrates regulate gamma-aminobutyric acid transporters in a syntaxin 1A-dependent manner. *Proc Natl Acad Sci U S A*, *99*(8), 5686–5691. https://doi.org/10.1073/pnas.082712899

Quick, M. W., Corey, J. L., Davidson, N., & Lester, H. A. (1997). Second messengers, trafficking-related proteins, and amino acid residues that contribute to the functional regulation of the rat brain GABA transporter GAT1. *J Neurosci*, *17*(9), 2967–2979. https://doi.org/10.1523/JNEUROSCI.17-09-02967.1997

Rossi, S., Muzio, L., De Chiara, V., Grasselli, G., Musella, A., Musumeci, G., Mandolesi, G., De Ceglia, R., Maida, S., Biffi, E., Pedrocchi, A., Menegon, A., Bernardi, G., Furlan, R., Martino, G., & Centonze, D. (2011). Impaired striatal GABA transmission in experimental autoimmune encephalomyelitis. *Brain, Behavior, and Immunity*, *25*(5), 947–956. https://doi.org/10.1016/j.bbi.2010.10.004

Rossi, S., Studer, V., Motta, C., De Chiara, V., Barbieri, F., Bernardi, G., & Centonze, D. (2012). Inflammation inhibits GABA transmission in multiple sclerosis. *Multiple Sclerosis Journal*, *18*(11), 1633–1635. https://doi.org/10.1177/1352458512440207

Schiavo, G., Shone, C. C., Bennett, M. K., Scheller, R. H., & Montecucco, C. (1995). Botulinum neurotoxin type C cleaves a single Lys-Ala bond within the carboxyl-terminal region of syntaxins. *J Biol Chem*, *270*(18), 10566–10570. https://doi.org/10.1074/jbc.270.18.10566

Schroder, K., Sweet, M. J., & Hume, D. A. (2006). Signal integration between IFN gamma and TLR signalling pathways in macrophages. *Immunobiology*, *211*(6-8), 511–524. https://doi.org/10.1016/j.imbio.2006.05.007

Song, Q., Pifferi, S., Shi, L., Chen, C., Proietti Zaccaria, R., Menini, A., Cao, J., Zhang, Q., & Torre, V. (2020). Textured nano fibrils drive microglial phenotype. *Biomaterials*, *257*, 120177. https://doi.org/10.1016/j.biomaterials.2020.120177

Su, J., Yin, J., Qin, W., Sha, S., Xu, J., & Jiang, C. (2015). Role for pro-inflammatory cytokines in regulating expression of GABA transporter type 1 and 3 in specific brain regions of kainic acid-induced status epilepticus.

Neuro chem Res, *40*(3), 621–627. https://doi.org/10.1007/s11064-014-1504-y

Thion, M. S., Ginhoux, F., & Garel, S. (2018). Microglia and early brain development: An intimate journey. *Science*, *362*(6411), 185–189. https://doi.org/10.1126/science.aat0474

Varoqueaux, F., Sigler, A., Rhee, J. S., Brose, N., Enk, C., Reim, K., & Rosenmund, C. (2002). Total arrest of spontaneous and evoked synaptic transmission but normal synaptogenesis in the absence of Munc 13-mediated vesicle priming. *Proc Natl Acad Sci U S A*, *99*(13), 9037–9042. https://doi.org/10.1073/pnas.122623799

Yan, X., Jiang, E., & Weng, H. R. (2015). Activation of toll like receptor 4 attenuates GABA synthesis and postsynaptic GABA receptor activities in the spinal dorsal horn via releasing interleukin-1 beta. *Journal of Neuro inflammation*, *12*(1). https://doi.org/10.1186/s12974-014-0222-3

SUPPORTING INFORMATION

Additional supporting information can be found online in the Supporting Information section at the end of this article.

How to cite this article: Di Palma, M., Catalano, M., Serpe, C., De Luca, M., Monaco, L., Kunzelmann, K., Limatola, C., Conti, F., & Fattorini, G. (2023). Lipopolysaccharide augments microglial GABA uptake by increasing GABA transporter-1 trafficking and bestrophin-1 expression. *Glia*, *71*(11), 2527–2540. https://doi.org/10.1002/glia.24437